

**Efficient computation of characteristic roots  
of delay differential equations using LMS  
methods**

*Koen Verheyden    Tatyana Luzyanina    Dirk Roose*

*Report TW 383, January 2004*



**Katholieke Universiteit Leuven**  
**Department of Computer Science**

Celestijnenlaan 200A – B-3001 Heverlee (Belgium)

# Efficient computation of characteristic roots of delay differential equations using LMS methods \*

*Koen Verheyden    Tatyana Luzyanina<sup>†</sup>    Dirk Roose*

*Report TW 383, January 2004*

Department of Computer Science, K.U.Leuven

## Abstract

We aim at the efficient computation of the rightmost characteristic roots of a system of delay differential equations. The approach we use is based on the discretization of the solution operator by linear multistep (LMS) methods. This results in an eigenvalue problem whose size is inversely proportional to the steplength used in the discretization. We use theoretical results on the location and numerical preservation of roots obtained in earlier work. Furthermore, we construct special-purpose LMS methods emphasising the accuracy of approximation of characteristic roots. We present a novel procedure that computes efficiently and accurately *all* roots in any right half-plane. In particular, no roots with large imaginary parts can be overlooked. The performance of the new procedure is demonstrated for small and large-scale systems of delay differential equations.

**Keywords :** delay differential equations, stability analysis, characteristic roots  
**AMS(MOS) Classification :** 65L06, 65L07, 65Q05

---

\* submitted for publication

<sup>†</sup>On leave from the Institute of Mathematical Problems in Biology, RAS, Pushchino, Moscow region, 142290, Russia.

# 1 Introduction

We consider a system of linear *delay differential equations* (DDEs) of the form

$$y'(t) = A_0 y(t) + \sum_{j=1}^m A_j y(t - \tau_j), \quad \text{where } y(t) \in \mathbb{R}^{n \times 1}, \quad (1.1)$$

with  $A_0, A_j \in \mathbb{R}^{n \times n}$  and *delays*  $\tau_j > 0$ , for  $j = 1, \dots, m$ . The stability (of the zero steady state solution) of (1.1) is determined by the *characteristic roots*  $\lambda$  of the *characteristic equation*

$$\det(\lambda I - A_0 - \sum_{j=1}^m A_j e^{-\lambda \tau_j}) = 0. \quad (1.2)$$

System (1.1) is asymptotically stable if all characteristic roots  $\lambda$  of (1.2) lie in the open left half-plane, i.e.,  $\Re(\lambda) < 0$ , see e.g. [11]. Note that (1.2) has an infinite number of roots  $\lambda$ . However, the number of roots in any right half-plane, i.e., with  $\Re(\lambda) \geq r \in \mathbb{R}$  is finite. Hence the stability of (1.1) is always determined by a finite number of roots.

Remark that system (1.1) can be considered as the linearization of the nonlinear DDE system

$$x'(t) = f(x(t), x(t - \tau_1), \dots, x(t - \tau_m)) \quad (1.3)$$

about a steady state solution  $x(t) \equiv x^*$ , where  $f(\cdot)$  is continuously differentiable. The *local stability* of the steady state  $x^*$  of (1.3) is determined by the stability of (1.1).

One approach to compute the rightmost characteristic roots of (1.2) is presented in [8] and implemented in the software package DDE-BIFTOOL [6, 7]. Other methods to study the stability of (1.2) are discussed in e.g. [13, 5]. The recent research focuses mainly on methods using discretizations of either the *solution operator* [8] or the *infinitesimal generator* [1, 2, 3] to (1.1). In [8], the solution operator is discretized using a *linear multistep* (LMS) method with polynomial interpolation to evaluate the delayed terms. The size of the resulting eigenvalue problem is inversely proportional to the steplength used in the discretization. The dominant eigenvalues,  $\tilde{\mu}$ , correspond (by an exponential transform) to  $\tilde{\lambda}$  which approximate the rightmost roots  $\lambda$  of (1.2). In [8], a heuristic choice of the steplength used in the discretization was proposed to approximate *all* roots  $\lambda$  with  $\Re(\lambda) \geq r$ . Remark that in [1, 2, 3] no heuristic is used to determine a priori a suitable fineness (or coarseness) of the discretization of the infinitesimal generator. Rather, the resulting accuracy is checked a posteriori by using Richardson extrapolation.

Using the procedure presented in [8], typically much more characteristic roots than desired are computed with a good accuracy.

In this paper we present a modification of the procedure described above. The novel procedure aims to reduce the computational cost while maintaining the reliability of the numerical results. We use theoretical foundations on the location and numerical preservation of roots obtained in [15]. Furthermore, we construct special-purpose LMS methods instead of using methods traditionally used for time integration. These techniques allow to define a novel heuristic resulting in a larger steplength, hence the size of the resulting eigenvalue problem is reduced. If this eigenvalue problem is still too large to be treated, it can be “split” into different smaller ones which “zoom in” on different pieces of (the interesting part of) the

complex plane. The resulting procedure computes efficiently and accurately *all* roots  $\lambda$  with  $\Re(\lambda) \geq r$ . In particular, no roots with large imaginary parts can be overlooked.

This paper is structured as follows. Section 2 summarizes the computation of the rightmost characteristic roots and the steplength heuristic of [8]. This section also contains results of [15] on the location and numerical preservation of roots. In Section 3 we derive special-purpose LMS methods. Section 4 presents the novel procedure to compute the rightmost characteristic roots. The significant reduction in computational cost is illustrated by examples in Section 5. In Section 6 we draw conclusions.

## 2 Preliminaries

Sections 2.1 and 2.2 summarize the computation of the rightmost characteristic roots and the steplength heuristic of [8], respectively. The latter section also argues why these techniques can be improved and outlines the way to achieve this goal. Next, Section 2.3 considers the theoretical foundation on the location and numerical preservation of roots [15] which we need.

### 2.1 Approximation of the rightmost characteristic roots

Let  $\mathbb{C}_0^+ := \{\lambda \in \mathbb{C} : \Re(\lambda) > 0\}$  and  $\mathbb{C}^+ := \{\lambda \in \mathbb{C} : \Re(\lambda) \geq 0\}$  denote the open and closed right half-plane, respectively. The definitions for the open and closed left half-plane,  $\mathbb{C}_0^-$  and  $\mathbb{C}^-$ , respectively, are analogous.

As detailed in [8], approximations to the characteristic roots  $\lambda$  can be obtained by first discretizing (1.1) using an LMS method coupled with polynomial interpolation to evaluate delayed terms. This discrete scheme is not used for time-stepping, but for the discretization of the solution operator over one time step (see below). A  $k$ -step LMS method is characterized by the function

$$\text{LMS}(z) := \frac{\alpha(e^z)}{\beta(e^z)}, \quad \text{with} \quad \alpha(e^z) := \sum_{i=0}^k \alpha_i (e^z)^i, \quad \beta(e^z) := \sum_{i=0}^k \beta_i (e^z)^i. \quad (2.1)$$

Let  $h$  be the steplength used in the discretization. A delayed term in (1.1),  $y(t_i - \tau_j)$ , is approximated by Lagrange interpolation, i.e.,

$$y(t_i - \tau_j) \approx \sum_{\ell=-s_-}^{s_+} \psi_\ell(\epsilon_j) y_{i+\ell-L_j}, \quad \text{with} \quad \psi_\ell(\epsilon_j) := \prod_{\substack{o=-s_-, o \neq \ell}}^{s_+} \frac{\epsilon_j - o}{\ell - o}, \quad (2.2)$$

where  $L_j := \lceil \tau_j/h \rceil$ ,  $\epsilon_j := L_j - \tau_j/h \in [0, 1[$  and  $s_- \leq s_+ \leq s_- + 2$ . As argued in [15], we bound the steplength  $h$  above by

$$h_{\max} := \tau_{\min}/s_+, \quad (2.3)$$

where  $\tau_{\min} := \min_j \tau_j$  is the minimal delay. Furthermore, we assume that  $\alpha(\cdot)$  and  $\beta(\cdot)$  in (2.1) are *irreducible*, such that there are no roots that are only caused by the LMS scheme.

The solution operator to (1.1) over one time step of length  $h$  is discretized by the scheme described above, cf. [8]. The resulting matrix has size  $N \times N$ , where

$$N := n(k + \lceil \tau_{\max}/h \rceil + s_-) \approx n\tau_{\max}/h, \quad (2.4)$$

with  $\tau_{\max} := \max_j \tau_j$ , the maximal delay. The dominant eigenvalues  $\tilde{\mu}$  of this matrix approximate the dominant eigenvalues  $\mu$  of the solution operator. By using  $\tilde{\mu} = e^{\tilde{\lambda}h}$  with  $|\Im(\tilde{\lambda})h| \leq \pi$ , approximations  $\tilde{\lambda}$  to roots  $\lambda$  of (1.2) are obtained.

Choose  $s_- + s_+ + 1 = p$ , where  $p$  is the order of the LMS method used. Then, the error  $|\tilde{\lambda} - \lambda|$  in approximating a root  $\lambda$  with multiplicity  $\nu$  behaves as  $h^{p/\nu}$ . In the package DDE-BIFTOOL [6, 7], the approximations  $\tilde{\lambda}$  are corrected by Newton iterations up to a desirable accuracy.

## 2.2 A steplength heuristic to obtain all roots in $\mathbb{C}^+ + r$

Let  $\sigma(\cdot)$  denote the spectrum of a matrix. Then, the characteristic equation (1.2) can be written as

$$\lambda \in \Sigma_\tau(\lambda) := \sigma(A_0 + \sum_{j=1}^m A_j e^{-\lambda\tau_j}). \quad (2.5)$$

In [8], a heuristic choice of the steplength used in the discretization, cf. Section 2.1, was presented to approximate all roots  $\lambda$  with  $\Re(\lambda) \geq r$ . This steplength heuristic was derived for LMS methods that have *property C* [10] and for which  $\text{LMS}(\mathbb{C}^+) \cap \text{LMS}(\mathbb{C}_0^-) = \emptyset$  holds, such as the *BDF* methods up to order 6. Note that Property C and the property of irreducibility imply that  $\text{LMS}(i[0, 2\pi])$  is the boundary of  $\text{LMS}(\mathbb{C}_0^-)$ .

The steplength heuristic in [8] was developed in two stages. Let  $\Sigma_\tau(\mathbb{D}) := \bigcup_{\lambda \in \mathbb{D}} \Sigma_\tau(\lambda)$  and  $|\mathbb{D}| := \{|c| : c \in \mathbb{D}\}$ , where  $\mathbb{D} \subseteq \mathbb{C}$ . First, the fact that  $\max |\Sigma_\tau(\mathbb{C}^+)| \leq \sum_{j=0}^m \|A_j\|$  was used. Let  $\rho_{\text{LMS},\epsilon}$  denote the radius of the disc in the complex plane centered at the origin in which  $\text{LMS}(i[0, 2\pi])$  approximates the imaginary axis up to some accuracy  $\epsilon > 0$ . For a more precise definition, see [8]. Then, the (open) right and left half-plane are approximated in this disc up to the accuracy  $\epsilon$  by  $\frac{1}{h}\text{LMS}(\mathbb{C}_0^+)$  and  $\frac{1}{h}\text{LMS}(\mathbb{C}_0^-)$ , respectively. Hence the steplength  $h$  given by

$$h = \frac{\rho_{\text{LMS},\epsilon}}{\sum_{j=0}^m \|A_j\|}, \quad (2.6)$$

scales  $\frac{1}{h}\text{LMS}(\cdot)$  such that the part of  $\Sigma_\tau(\mathbb{C}^+)$  located in  $\mathbb{C}^+ + \epsilon/h$  is included in  $\frac{1}{h}\text{LMS}(\mathbb{C}_0^+)$ . Likewise, the part of  $\Sigma_\tau(\mathbb{C}^+)$  located in  $\mathbb{C}^- - \epsilon/h$  is included in  $\frac{1}{h}\text{LMS}(\mathbb{C}_0^-)$ . This is illustrated in Fig. 1 (right). It can be proven that, by the above choice of the steplength, the delay-independent stability and instability of (1.1) are recovered up to the given  $\epsilon$ .

Next, a heuristic choice of  $h$  was proposed to approximate roots  $\lambda \in \mathbb{C}^+ + r$ :

$$h = 0.9 \frac{\rho_{\text{LMS},\epsilon}}{\|A_0\| + |r| + \sum_{j=1}^m \|A_j\| e^{-r\tau_j}}, \quad (2.7)$$

where 0.9 is a safety factor. This heuristic is implemented in DDE-BIFTOOL. Since the eigenvalues of the discretization of the solution operator have approximately the same modulus, they are computed using the QR method. However, its cost grows like  $N^3 \approx n^3(\tau_{\max}/h)^3$ .

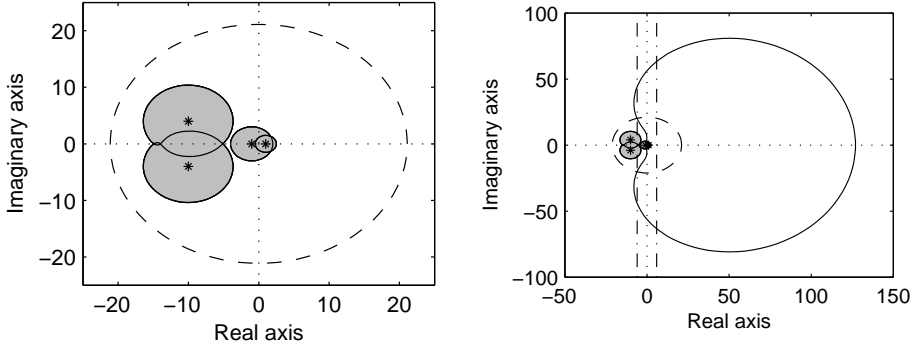


Figure 1: For the DDE system in Section 5.1 with  $n = 4$  and  $m = 1$ :  $\text{cl } \Sigma_\tau(\mathbb{C}^+) = \Omega(\mathbb{R}^+ \vec{\tau}) \cup \sigma(A_0)$  (colored in gray),  $\Omega(\vec{0})$  (solid line), the eigenvalues of  $A_0$  (\*) and the circle around the origin with radius  $\sum_{j=0}^m \|A_j\|$  (dashed line). Right:  $\frac{1}{h}\text{LMS}(i[0, 2\pi[)$ , where  $h$  is given by (2.6) (solid line) and parallel lines,  $\pm\epsilon/h$  from the imaginary axis (dash-dotted lines), in case of the BDF method of 4<sup>th</sup> order (with a rather large  $\epsilon$  for visibility).

Our experiments with heuristic (2.7) show that it leads to a good approximation of more characteristic roots than desired, i.e., all  $\lambda$  in  $\mathbb{C}^+ + R$ , where  $R < r$  are approximated well, see e.g. Fig. 5.3 in [8]. Note that the steplength heuristic should only “guarantee” that the wanted roots are approximated with sufficient accuracy so that the subsequent Newton iterations will converge successfully. Clearly, it would be advantageous to obtain a novel heuristic which allows to use a larger steplength.

Heuristic (2.7) usually results in a steplength  $h$  that is much smaller than necessary. This is mainly due to the denominator in (2.7) which is an upper bound for  $|r| + \max |\Sigma_\tau(\mathbb{C}^+ + r)|$ . This upper bound typically overestimates  $\max |\Sigma_\tau(\mathbb{C}^+ + r) \cap (\mathbb{C}^+ + r)|$ , see Fig. 1 (left), where  $r = 0$ . The latter quantity is important since, by (2.5), the roots  $\lambda$  that lie in  $\mathbb{C}^+ + r$  are included in  $\Sigma_\tau(\mathbb{C}^+ + r)$ . Hence heuristic (2.7) overestimates the extent of the spectrum in  $\mathbb{C}^+ + r$ . This suggests one way to optimize this heuristic: considering more precisely the location of  $\Sigma_\tau(\mathbb{C}^+ + r)$  w.r.t.  $\mathbb{C}^+ + r$ . The second way is to reconsider the properties of LMS methods that are desirable for our purpose. It will be clarified that other requirements have to be imposed on the LMS methods used. This results in the construction of special-purpose LMS methods. The first way, i.e., locating  $\Sigma_\tau(\mathbb{C}^+ + r)$  w.r.t.  $\mathbb{C}^+ + r$ , is considered in the next section, while in Section 3, special-purpose LMS methods are constructed. Combining both ideas will lead to a novel steplength heuristic of a totally different form as heuristic (2.7). These new techniques are worked out in Section 4, where they are combined in a novel procedure to compute *all* characteristic roots in  $\mathbb{C}^+ + r$ .

### 2.3 The location and numerical preservation of roots

This section summarizes the work on the location and numerical preservation of roots in [15]. These results allow to consider more precisely the location of  $\Sigma_\tau(\mathbb{C}^+ + r)$  w.r.t.  $\mathbb{C}^+ + r$ . Moreover, the results on the numerical preservation of characteristic roots motivate (partially) the requirements for the special-purpose

LMS methods constructed in Section 3.

First the location of the characteristic roots in the complex plane is considered. Let  $\vec{\tau} := (\tau_1, \dots, \tau_m)$  and denote by  $\Omega(\cdot; \vec{\tau})$  the set-valued function that maps  $\xi \in \mathbb{R}$  unto

$$\Omega(\xi; \vec{\tau}) := \bigcup_{\vec{\omega} \in [0, 2\pi]^m} \sigma(A_0 + \sum_{j=1}^m A_j e^{-(\xi\tau_j + i\omega_j)}). \quad (2.8)$$

Let  $(\mathbb{R}^+ + r)\vec{\tau} := \{\xi\vec{\tau} : \xi \geq r\}$  and denote by “cl” the closure. The set  $\Omega(r\vec{\tau})$  encloses (or encircles) the region  $\Omega((\mathbb{R}^+ + r)\vec{\tau}) \cup \sigma(A_0) = \text{cl } \Sigma_\tau(\mathbb{C}^+ + r)$ . Hence  $\Omega(r\vec{\tau}) \cap (\mathbb{C}^+ + r)$  encloses a region that contains *all* roots  $\lambda$  in  $\mathbb{C}^+ + r$ .

Moreover, in [15], a decomposition  $\Omega(\cdot; \vec{\tau}) \equiv \bigcup_{i=1}^n \Omega_i(\cdot; \vec{\tau})$  is constructed. The resulting “ $\Omega_i((\mathbb{R}^+ + r)\vec{\tau})$ -regions” can partially or totally overlap. This is illustrated in Fig. 1 (left). In this case,  $n = 4$ , while there are only three distinct  $\Omega_i((\mathbb{R}^+ + r)\vec{\tau})$ -regions (for  $r = 0$ ). The largest  $\Omega_i(\mathbb{R}^+ \vec{\tau})$ -region is obtained two times. Notice that in the case of commensurate delays or a single delay (cf. Fig. 1), the sets  $\Omega_i(r\vec{\tau})$  are curves.

Let us turn to the numerical preservation of characteristic roots. Consider the discrete approximation to the characteristic equation (2.5) that is presented in Section 2.1. As detailed in [8, 15], the stability of this discrete scheme is determined by the real parts of the roots  $\tilde{\lambda}$  satisfying

$$\frac{1}{h} \text{LMS}(\tilde{\lambda}h) \in \Sigma_{\tau,h}(\tilde{\lambda}) := \sigma\left(A_0 + \sum_{j=1}^m A_j e^{-\tilde{\lambda}\tau_j} \sum_{\ell=-s_-}^{s_+} \psi_\ell(\epsilon_j) e^{\tilde{\lambda}(\ell-\epsilon_j)h}\right), \quad (2.9)$$

and  $|\Im(\tilde{\lambda})| \leq \pi/h$ . Comparing the right hand sides of (2.5) and (2.9), one observes that  $\Sigma_{\tau,h}(\cdot) \approx \Sigma_\tau(\cdot)$ . In the case of commensurate delays, it is possible to eliminate the use of interpolation (2.2) in the discrete approximation, such that  $\Sigma_{\tau,h}(\tilde{\lambda}) \equiv \Sigma_\tau(\tilde{\lambda})$ . In order to evaluate the influence of the interpolation on the preservation of characteristic roots, we define the set  $\Psi$  as

$$\Psi := \left\{ \tilde{\lambda} \in \mathbb{C} : r \leq \Re(\tilde{\lambda}) - \frac{1}{\tau_j} \log \left| \sum_{\ell=-s_-}^{s_+} \psi_\ell(\epsilon_j) e^{\tilde{\lambda}(\ell-\epsilon_j)h} \right|, \text{ for } j = 1, \dots, m \right\}, \quad (2.10)$$

which is a function of  $r$ ,  $\vec{\tau}$ ,  $h$ ,  $s_-$  and  $s_+$ . Due to the quality of the polynomial interpolation,  $\mathbb{C}^+ + r$  is approximated well by  $\Psi$ . In case no interpolation is performed (i.e.,  $\epsilon_j \equiv 0$ ),  $\Psi = \mathbb{C}^+ + r$ , by (2.10).

Denote by  $\vec{\tau} > \vec{0}$  that  $\tau_j > 0$ , for  $j = 1, \dots, m$ . The following result on the preservation of characteristic roots in  $\mathbb{C}^+ + r$  holds.

**Theorem 2.1.** (Theorem 4.2 in [15]) Let  $r \in \mathbb{R}$ ,  $\vec{\tau} > \vec{0}$ ,  $h \in ]0, h_{\max}]$  (cf. (2.3)) and  $s_- \leq s_+ \leq s_- + 2$ .

(i) Let  $\Omega(r\vec{\tau}) \cap (\mathbb{C}^+ + r) = \emptyset$ . Then

- (1.2) has no roots  $\lambda$  in  $\mathbb{C}^+ + r$  and
- (2.9) has no roots  $\tilde{\lambda}$  in  $\Psi$  that satisfy  $\frac{1}{h} \text{LMS}(h\tilde{\lambda}) \in \mathbb{C}^+ + r$ .

(ii) Let  $\Psi_\circ \subseteq \Psi$  be multiple connected. Assume there are  $n_r$   $\Omega_i(r\vec{\tau})$ -regions that lie in  $\mathbb{C}_0^+ + r$ . If those  $\Omega_i(r\vec{\tau})$ -regions also lie in the interior of  $\frac{1}{h} \text{LMS}(h\Psi_\circ)$ , then

- (1.2) has at least  $n_r$  roots  $\lambda$  (counting multiplicities) that lie in the interior of  $(\mathbb{C}_0^+ + r) \cap \frac{1}{h}\text{LMS}(h\Psi_\circ)$  and
- those roots are approximated by  $n_r$  roots  $\tilde{\lambda}$  (counting multiplicities) of (2.9) that lie in the interior of  $\Psi_\circ$ .

The preservation of (in-)stability, i.e.  $r = 0$ , is now treated in more detail. We first define the *stability preserving region* of an LMS method as

$$\mathcal{S}_{\text{pr}}^+ := \{z \in \mathbb{C}^+ : \text{LMS}(z) \in \mathbb{C}^+\}. \quad (2.11)$$

This region (2.11) is the domain where  $\text{LMS}(\cdot)$  “maps unstable points on unstable points”. The stability preserving region differs from the stability region of an LMS method, defined as the subset of the complex plane where no  $\lambda \in \mathbb{C}_0^+$  are mapped upon by  $\text{LMS}(\cdot)$ . For a more precise definition of the latter, see e.g. [10]. The following (delay-independent) result holds.

**Corollary 2.1.** (Corollary 4.1 in [15]) *Under the assumptions of Theorem 2.1, the following holds.*

- If  $\Omega(\vec{0}) \cap \mathbb{C}^+ = \emptyset$ , then (1.2) has no roots  $\lambda \in \mathbb{C}^+$  and (2.9) has no roots in  $\frac{1}{h}\mathcal{S}_{\text{pr}}^+ \subset \mathbb{C}^+$  for all  $\vec{\tau} > \vec{0}$ .
- Assume that  $n_r$   $\Omega_i(\vec{0})$ -regions lie in the interior of  $\frac{1}{h}\text{LMS}(\mathcal{S}_{\text{pr}}^+) \subset \mathbb{C}_0^+$ . Then (1.2) has at least  $n_r$  roots  $\lambda$  (counting multiplicities) in the interior of  $\frac{1}{h}\text{LMS}(\mathcal{S}_{\text{pr}}^+)$  and those roots are approximated by  $n_r$  roots  $\tilde{\lambda}$  (counting multiplicities) of (2.9) that lie in the interior of  $\frac{1}{h}\mathcal{S}_{\text{pr}}^+ \subset \mathbb{C}^+$  for all  $\vec{\tau} > \vec{0}$ .

Hence, under the appropriate conditions, the stability properties are maintained inside the scaled stability preserving region  $\frac{1}{h}\mathcal{S}_{\text{pr}}$ .

### 3 Special-purpose LMS methods

As foreshadowed at the end of Section 2.2, the properties of LMS methods that are desirable for our purpose to approximate accurately the rightmost roots (i.e., those in  $\mathbb{C}^+ + r$  for a given  $r \in \mathbb{R}$ ) have to be considered in detail. These desired properties are derived in Section 3.1. Next, in Section 3.2, we construct special-purpose LMS methods.

#### 3.1 The requirements on the discrete approximation

##### 3.1.1 Approximation of the characteristic equation

This section considers the role of the LMS method in the approximation of the characteristic equation (2.5) by (2.9).

Denote by  $\sigma_i(\cdot)$  an element of the set in the right hand side of (2.5), for  $i = 1, \dots, n$ . Note that the continuity of  $\sigma_i(\cdot)$  is considered in more detail in [15]. Let  $\lambda$  be a characteristic root such that  $\lambda = \sigma_i(\lambda)$  for some  $i$ . Let the multiplicity of  $\lambda$  equal  $\nu$  and let  $\tilde{\lambda} \approx \lambda$ . Hence, it follows from the Taylor expansion that  $\sigma_i(\tilde{\lambda}) - \tilde{\lambda} \approx \kappa_i^{-1}(\lambda)(\tilde{\lambda} - \lambda)^\nu$ , where

$$\kappa_i(\lambda) := \begin{cases} (\sigma_i'(\lambda) - 1)^{-1}, & \text{if } \nu = 1, \\ \nu!(\sigma_i^{(\nu)}(\lambda))^{-1}, & \text{otherwise.} \end{cases} \quad (3.1)$$

We neglect the influence of the interpolation in (2.9), such that  $\frac{1}{h}\text{LMS}(\tilde{\lambda}h)$  equals  $\sigma_i(\tilde{\lambda})$ . Combining the above implies that

$$\tilde{\lambda} - \lambda \approx \left[ \kappa_i(\lambda) \left( \frac{1}{h}\text{LMS}(\tilde{\lambda}h) - \tilde{\lambda} \right) \right]^{1/\nu}. \quad (3.2)$$

The error estimation in (3.2) motivates the following definition of the “*trust-region*”  $\mathcal{T}_\delta$  for a given *relative tolerance*  $\delta > 0$ .

$$\mathcal{T}_\delta := \left\{ z \in \mathbb{C}_0^- \cup \mathcal{S}_{\text{pr}}^+ : |\Im(z)| < \pi, \quad |\text{LMS}(z) - z| \leq \delta|z| \right\}. \quad (3.3)$$

The occurrence of  $\mathcal{S}_{\text{pr}}^+$  in definition (3.3) will be clarified in Section 3.1.2. We may expect that the  $\tilde{\lambda}$  that lie in  $\frac{1}{h}\mathcal{T}_\delta$  are good approximations to characteristic roots  $\lambda$  of (1.2). Indeed, assume that a simple root  $\lambda$  is approximated by a  $\tilde{\lambda}$  at the boundary of  $\frac{1}{h}\mathcal{T}_\delta$ . Then, by 3.2, the relative error  $|\tilde{\lambda} - \lambda|/|\tilde{\lambda}|$  is approximately  $|\kappa_i(\lambda)|\delta$ , for some  $i \in \{1, \dots, n\}$ . It is illustrated in Section 3.2 that the origin belongs to  $\mathcal{T}_\delta$  for all  $\delta > 0$ . Thus, the smallest error can be expected for  $\tilde{\lambda}$  close to the origin.

### 3.1.2 The preservation of roots

We now discuss the practical use of the results of Section 2.3 on the numerical preservation of characteristic roots.

Recall that, the “*heuristic tolerance*” implied by (3.3) holds for all approximate roots  $\tilde{\lambda} \in \frac{1}{h}\mathcal{T}_\delta$ . For this purpose, it is important that the regions  $\mathcal{T}_\delta$  and  $\text{LMS}(\mathcal{T}_\delta)$  are large. Clearly, a large  $\text{LMS}(\mathcal{T}_\delta)$  is also beneficial for the results of Section 2.3. Indeed, assume that the  $\text{LMS}(\cdot)$ -mapping approximates the identity mapping in a large part of the complex plane. Then  $\frac{1}{h}\text{LMS}(h\tilde{\lambda})$  in Theorem 2.1 is approximated well by  $\tilde{\lambda}$ , even for a large steplength  $h$ . The latter obviously goes together with a large stability preserving region  $\mathcal{S}_{\text{pr}}^+$ .

First consider the preservation of (in-)stability, i.e., the case  $r = 0$ , covered by Corollary 2.1. By (3.3),  $\mathcal{T}_\delta$  is chosen such that  $\mathcal{T}_\delta \cap \mathbb{C}^+ \subseteq \mathcal{S}_{\text{pr}}^+$ . We assume that  $\text{LMS}(\mathcal{T}_\delta) \cap \mathbb{C}^+ \subseteq \text{LMS}(\mathcal{S}_{\text{pr}}^+)$ . The latter property holds if  $\delta$  is sufficiently small, which is true in practice, cf. the figures in the next section. Let  $h$  be chosen such that the part of  $\Omega(\vec{0})$  that lies in  $\mathbb{C}^+$  also belongs to  $\frac{1}{h}\text{LMS}(\mathcal{T}_\delta)$ . Then the stability properties are preserved inside  $\frac{1}{h}\mathcal{T}_\delta$  in the sense of Corollary 2.1. In case  $\text{LMS}(\mathcal{S}_{\text{pr}}^+)$  contains part of the imaginary axis there is no need for an  $\epsilon$  with a similar meaning as in heuristic (2.7). Therefore we require that the  $\text{LMS}(\cdot)$  function maps a line segment  $i] - \vartheta, \vartheta[$  with  $\vartheta > 0$  onto the imaginary axis. Assuming that  $\text{LMS}(\cdot)$  has no *poles* on  $i] - \pi, \pi[$ , this condition is equivalent to

$$\text{LMS}(i] - \pi, \pi[) \subseteq i\mathbb{R}, \quad (3.4)$$

by analyticity. Clearly, this property is also desirable for the approximate preservation of Hopf bifurcations.

In the general case  $r \neq 0$ , one has to consider the location of  $\Omega(r\vec{\tau}) \cap (\mathbb{C}^+ + r)$  w.r.t.  $\frac{1}{h}\text{LMS}(h\Psi_\circ)$ , where  $\Psi_\circ \subseteq \Psi$ . Assume that  $h$  is chosen such that the part of  $\Omega(r\vec{\tau})$  that lies in  $\mathbb{C}^+ + r$  also belongs to  $\frac{1}{h}\text{LMS}(h\Psi_\circ)$ . Here we choose  $\Psi_\circ = \frac{1}{h}\mathcal{T}_\delta \cap \Psi$  such that the approximations  $\tilde{\lambda}$  to the roots  $\lambda \in \mathbb{C}^+ + r$  belong to  $\frac{1}{h}\mathcal{T}_\delta$ . The

set  $\frac{1}{h}\text{LMS}(\mathcal{T}_\delta \cap h\Psi)$  depends on the chosen  $r$  in a way that is not straightforward. This set can be approximated by  $\frac{1}{h}\text{LMS}(\mathcal{T}_\delta) \cap (\mathbb{C}^+ + r - \Delta r)$ , which depends on  $r$  in an easy manner. Here,  $\Delta r \geq 0$  is a *safety margin*. The quality of this approximation is guaranteed by the good approximation of  $\mathbb{C}^+ + r$  by  $\Psi$ .

Assume that the safety margin  $\Delta r$  is “large enough”. Then  $\frac{1}{h}\mathcal{T}_\delta$  contains approximations  $\tilde{\lambda}$  to all rightmost characteristic roots  $\lambda \in \mathbb{C}^+ + r$ . The results (3.2) and (3.3) give confidence in these approximations.

### 3.2 Construction of special-purpose LMS methods

Our objective of approximating the roots in  $\mathbb{C}^+ + r$  imposes other requirements on LMS methods than in case of time integration. The desired properties were discussed in the previous section. Specifically, the size and extent of the stability region of the LMS method used is not important for our purpose. In the context of time integration, on the contrary, the stability region is important since it indicates which steplengths prevent that spurious modes due to the numerical scheme arise (and grow). However, in computing the eigenvalues using the QR algorithm, these spurious modes cannot grow to domination over the other modes. For our purpose, it is not the stability region, but the stability preserving region  $\mathcal{S}_{\text{pr}}^+$  and the trust-region  $\mathcal{T}_\delta$  which are important.

Some other properties are not required either. Specifically, Property C and the condition that  $\text{LMS}(\mathbb{C}^+) \cap \text{LMS}(\mathbb{C}_0^-) = \emptyset$ , which are used in [8], cf. Section 2.2, are not needed and hence they are not imposed.

Let us now concentrate on the desired properties. To obtain a large region  $\mathcal{T}_\delta$ , hence a large  $\text{LMS}(\mathcal{T}_\delta)$ , an LMS method of high order (and with small *error constant*  $C_{\text{err}}$ ) is potentially suitable. Indeed, in case of an irreducible and consistent LMS method of order  $p \geq 1$ , the  $\text{LMS}(\cdot)$ -mapping approximates the identity mapping in the neighborhood of the origin as

$$\text{LMS}(z) = z + C_{\text{err}}z^{p+1} + \mathcal{O}(z^{p+2}), \quad z \rightarrow 0.$$

This follows from the order condition which requires that

$$\alpha(e^z) - z\beta(e^z) = \beta(1)C_{\text{err}}z^{p+1} + \mathcal{O}(z^{p+2}), \quad z \rightarrow 0, \quad (3.5)$$

where  $\beta(1) \neq 0$ , see e.g. [9].

Thus we aim at methods of the highest order possible for a given number of steps  $k$  and satisfying (3.4). There remain  $2k + 1$  degrees of freedom in choosing LMS coefficients after the normalization  $\alpha_k = 1$ , cf. (2.1). By the linear independence of the functions  $z^d e^{\ell z}$ , for  $d \in \{0, 1\}$  and  $\ell \in \{0, \dots, k\}$ , at most  $2k + 1$  coefficients in the Taylor expansion of the left hand side of the order condition (3.5) can be set to zero. Hence  $p_{\text{max}} = 2k$  is the highest possible order.

The  $\text{LMS}(\cdot)$ -mapping is symmetric w.r.t. the real axis, just as  $\Sigma_\tau(\cdot)$  and  $\Omega(\cdot)$ . A sufficient condition to satisfy (3.4) is that the  $\text{LMS}(\cdot)$ -mapping is symmetric w.r.t. the imaginary axis as well or, equivalently, that this function is odd. One can obtain the latter by choosing  $\alpha_i = -\alpha_{k-i}$  and  $\beta_i = \beta_{k-i}$  for  $i = 0, \dots, \lfloor k/2 \rfloor$ . Indeed, using trigonometric identities, one immediately sees that  $\alpha(e^z)$  and  $\beta(e^z)$

$k$	$2k$	$\alpha_i$					$\beta_i$					$C_{\text{err}}$	$M_{\mathfrak{S}}$
2	4	-1	0	1			$\frac{1}{3}$	$\frac{4}{3}$	$\frac{1}{3}$			$-\frac{1}{180}$	$\sqrt{3}$
3	6	-1	$-\frac{27}{11}$	$\frac{27}{11}$	1		$\frac{3}{11}$	$\frac{27}{11}$	$\frac{27}{11}$	$\frac{3}{11}$		$-\frac{1}{2800}$	$+\infty$
4	8	-1	$-\frac{32}{5}$	0	$\frac{32}{5}$	1	$\frac{6}{25}$	$\frac{96}{25}$	$\frac{216}{25}$	$\frac{96}{25}$	$\frac{6}{25}$	$-\frac{1}{44100}$	2.20

Table 1: The LMS coefficients (listed in ascending order),  $C_{\text{err}}$  (computed using MAPLE) and  $M_{\mathfrak{S}}$  for three special-purpose LMS methods with  $k$  steps and order  $2k$ .

then have the form

$$\begin{aligned}\alpha(e^z) &= 2e^{\frac{k}{2}z} \left( \sinh\left(\frac{k}{2}z\right) - \alpha_1 \sinh\left(\frac{(k-2)}{2}z\right) - \dots - \alpha_{(k-1)/2} \sinh\left(\frac{z}{2}\right) \right), \\ \beta(e^z) &= 2e^{\frac{k}{2}z} \left( \beta_0 \cosh\left(\frac{k}{2}z\right) + \beta_1 \cosh\left(\frac{(k-2)}{2}z\right) + \dots + \beta_{k/2} \cosh\left(\frac{z}{2}\right) \right),\end{aligned}\tag{3.6}$$

where  $\alpha_{(k-1)/2} = 0$  for  $k$  even and  $k = 1$  and  $\beta_{k/2} = 0$  for  $k$  odd. Now consider the function  $e^{-\frac{k}{2}z}(\alpha(e^z) - z\beta(e^z))$ , which is odd by (3.6). Hence its Taylor expansion reads as

$$e^{-\frac{k}{2}z}(\alpha(e^z) - z\beta(e^z)) = \gamma_1 z + \gamma_2 z^3 + \dots + \gamma_k z^{2k-1} + \mathcal{O}(z^{2k+1}), \quad z \rightarrow 0, \tag{3.7}$$

where  $\gamma_1, \dots, \gamma_k$  are linear in the  $k$  free coefficients. It follows from comparison of (3.7) with the order condition (3.5) that the  $k$  equalities  $\gamma_1 = 0, \dots, \gamma_k = 0$  uniquely determine an LMS method of order  $p = 2k$ .

Summarizing, the above procedure constructs the (unique)  $k$ -step LMS method of maximal order  $2k$  satisfying  $\text{LMS}(i] - \pi, \pi[) \subseteq i\mathbb{R}$  for any integer  $k \geq 1$ . For  $k = 1$ , one obtains the *trapezoidal rule* of 2<sup>nd</sup> order. For the examples in Section 5 we used methods of 4<sup>th</sup>, 6<sup>th</sup> and 8<sup>th</sup> order, hence  $k = 2, 3$  and 4, respectively, see Table 1. This table also lists the remarkably small error constants of these special-purpose LMS methods and  $M_{\mathfrak{S}} := \sup \mathfrak{S}(\text{LMS}(i] - \pi, \pi[))$ . In the case  $k = 3$ ,  $M_{\mathfrak{S}} = +\infty$  since  $\text{LMS}(z)$  has a pole at  $z = i(2\ell + 1)\pi$  for  $\ell \in \mathbb{Z}$ . Note that for all methods listed in Table 1,  $\text{LMS}(\cdot)$  has no poles on  $i] - \pi, \pi[$ . Furthermore, these methods satisfy the irreducibility requirement, which we also need in Section 2.1.

In the above construction, we have not imposed that the origin is part of the stability region of the LMS method, which is called *zero-stability* (or *D-stability*). Dropping this requirement allows to circumvent the first Dahlquist barrier [9], which implies that the highest possible order of a zero-stable  $k$ -step LMS method is  $k + 2$  if  $k$  is even and  $k + 1$  if  $k$  is odd. Note that the zero-stable methods of highest order and even  $k$  also have the form (3.6). The special-purpose method of 4<sup>th</sup> order is called the *Milne-Simpson* method. It is also the zero-stable LMS method of order  $p \geq 2$  where  $M_{\mathfrak{S}}$  is maximal, see [10].

Remark that the stability region for the Milne-Simpson method is merely the interval  $i[-\sqrt{3}, \sqrt{3}]$ , while for the special-purpose methods of 6<sup>th</sup> and 8<sup>th</sup> order it is empty. However, as argued above, not the stability region, but the stability preserving region  $\mathcal{S}_{\text{pr}}^+$ , the trust-region  $\mathcal{T}_{\delta}$  and  $\text{LMS}(\mathcal{T}_{\delta})$  are important for our purpose.

The location of  $\mathcal{S}_{\text{pr}}^+$ ,  $\mathcal{T}_{\delta}$  and  $\text{LMS}(\mathcal{T}_{\delta})$  for  $\delta = 0.1$  for the special-purpose methods listed in Table 1 is shown in Fig. 2. Note that for the method of 6<sup>th</sup> order,

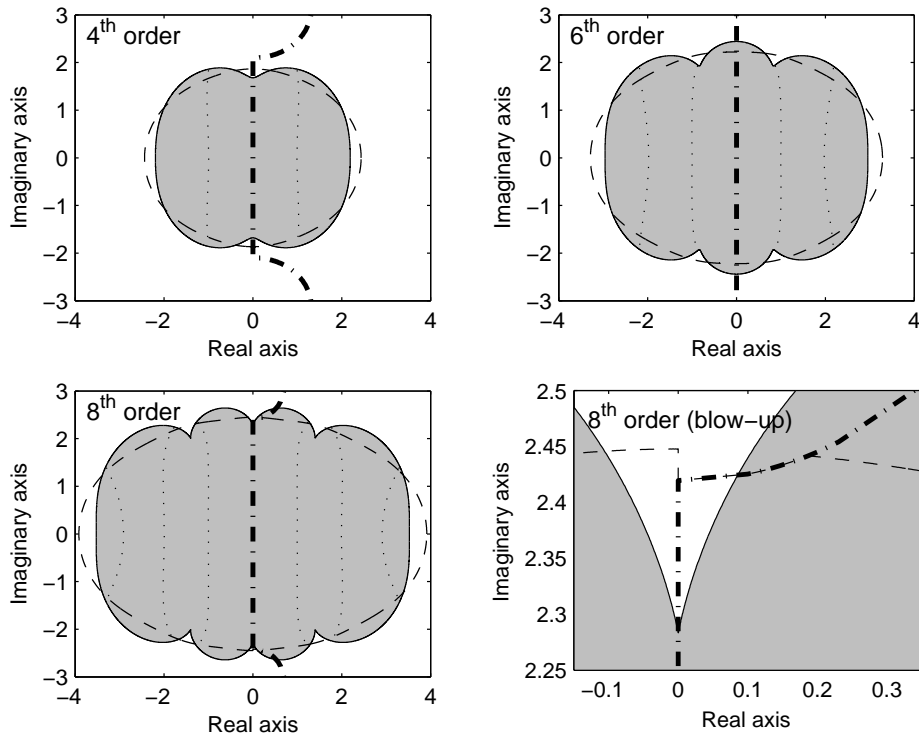


Figure 2:  $\mathcal{S}_{\text{pr}}^+$  (bounded by the thick dash-dotted line),  $\mathcal{T}_\delta$  for  $\delta = 0.1$  (bounded by the dashed line),  $\text{LMS}(\mathcal{T}_\delta)$  (colored in gray and bounded by the solid line) and (a part of) the image of lines parallel to the imaginary axis (with integer  $\Re(\cdot)$ ) under  $\text{LMS}(\cdot)$  (dotted lines) in case of the special-purpose methods of 4<sup>th</sup>, 6<sup>th</sup> and 8<sup>th</sup> order.

$\mathcal{S}_{\text{pr}}^+$  is large but does not equal  $\mathbb{C}^+$ . This figure also shows (a part of) the image of lines parallel to the imaginary axis under the  $\text{LMS}(\cdot)$ -mapping. These curves illustrate that the  $\text{LMS}(\cdot)$ -mapping indeed approximates the identity mapping well in a large region around the origin. For the method of 8<sup>th</sup> order, the blow-up in Fig. 2 (right, bottom) clearly shows that  $\mathcal{T}_\delta \cap \mathbb{C}^+ \subseteq \mathcal{S}_{\text{pr}}^+$  holds, cf. (3.3), as in the other cases.

Figs. 2 and 3 illustrate that  $\text{LMS}(\mathcal{T}_\delta)$  in case of the special-purpose methods is significantly larger than for other LMS methods of the same order, e.g. the BDF methods. This goes together with the remarkably small error constants of the special-purpose methods, cf. Table 1. Clearly, the latter is also important for the constant factor in the asymptotic result concerning the accuracy, cf. Section 2.1. By construction of the special-purpose methods,  $\text{LMS}(\mathcal{S}_{\text{pr}}^+)$  and  $\text{LMS}(\mathcal{T}_\delta)$  contain part of the imaginary axis. Remark that this property, which we need, cf. Section 3.1.2, does not hold for the BDF methods.

## 4 The novel procedure

In this section, we describe the building blocks of the novel procedure to compute *all* rightmost characteristic roots in  $\mathbb{C}^+ + r$  efficiently and with a good accuracy. Section 4.1 treats the novel steplength heuristic for the special-purpose LMS meth-

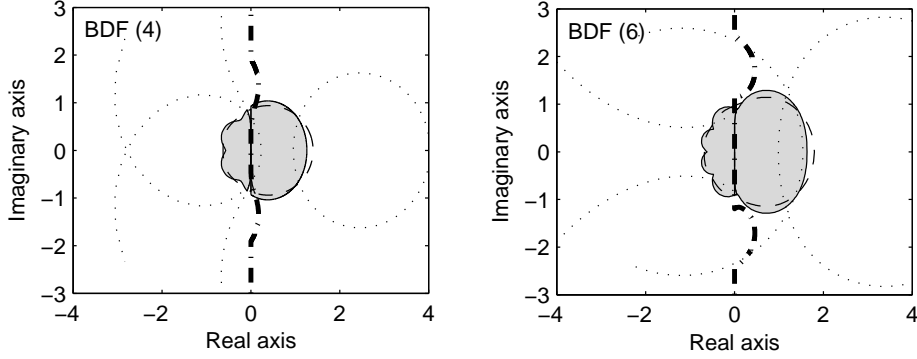


Figure 3: The same regions as in Fig. 2, but in case of the BDF methods of 4<sup>th</sup> and 6<sup>th</sup> order.

ods. This novel heuristic gives a larger steplength than heuristic (2.7) for any DDE system. Section 4.2 describes an alternative if the resulting eigenvalue problem remains too large to be treated by the QR method. Finally, Section 4.3 describes how the location of  $\Omega(r\vec{\tau})$  can be estimated, which is needed to calculate the heuristic steplength.

#### 4.1 The novel steplength heuristic

As argued in Section 3.1, we determine  $h$  such that the part of  $\Omega(r\vec{\tau})$  that lies in  $\mathbb{C}^+ + (r - \Delta r)$  also belongs to  $\frac{1}{h}\text{LMS}(\mathcal{T}_\delta)$ . Here,  $\Delta r \geq 0$  is a safety margin and  $\delta > 0$  is a relative tolerance. The region  $\text{LMS}(\mathcal{T}_\delta)$  for special-purpose LMS methods of different order is colored in gray in Fig 2. For practical use, instead of  $\text{LMS}(\mathcal{T}_\delta)$ , we consider regions whose form is more easy to handle and that are inscribed in  $\text{LMS}(\mathcal{T}_\delta)$ . In particular, we work with inscribed ellipses of the form

$$(\Re(z)/a_{\text{ell}})^2 + (\Im(z)/b_{\text{ell}})^2 = 1, \quad (4.1)$$

where  $a_{\text{ell}}$  and  $b_{\text{ell}}$  are determined for a given order and  $\delta > 0$  such that the ellipse has a large value of either  $a_{\text{ell}}$  or  $b_{\text{ell}}$ . Note that, in general, a large value of  $b_{\text{ell}}$  is preferable to a large  $a_{\text{ell}}$  by the typical wedge-like form of the rightmost part of  $\Omega((\mathbb{R}^+ + r)\vec{\tau})$ . Table 2 contains the parameters  $a_{\text{ell}}$  and  $b_{\text{ell}}$  of the ellipse (4.1) for three special-purpose LMS methods, in case of  $\delta = 0.1$  (cf. Fig 2). Note that for the 6<sup>th</sup> order method, two alternatives are given. In the remainder we only use the first one, because it gave the best results in almost all our computations, as expected. Remark that using ellipses rather than circles is certainly advantageous in this case since  $b_{\text{ell}}$  exceeds  $\text{rad}_{\text{circ}}$ .

Our heuristic choice of the steplength is formulated as follows. First, a (finite) set of points  $\{q_K \in \Omega(r\vec{\tau}) : K = 1, \dots\}$  is computed (cf. Section 4.3) for a given value of  $r$ . Ideally, one should have some confidence that these points are well spread out over  $\Omega(r\vec{\tau})$ . Next, we use the subset of the above points with real parts larger than  $r - \Delta r$  for some  $\Delta r > 0$ . We use the safety margin  $\Delta r$  for the reason explained in Section 3.1.2 and because only a limited number of points is computed. Finally, the largest value of  $h$  is determined such that the latter points

order	4	6	8
$a_{\text{ell}}$	2.193	1.345 2.958	3.523
$b_{\text{ell}}$	1.679	2.442 2.010	2.205
$\text{rad}_{\text{circ}}$	1.679	2.1000	2.205

Table 2: The parameters of ellipses (4.1) inscribed in  $\text{LMS}(\mathcal{T}_\delta)$  for  $\delta = 0.1$  and  $\text{rad}_{\text{circ}}$ , the radius of the largest inscribed circle centered around the origin.

(or its convex hull) scaled by a factor  $h/0.9$  fit into an ellipse of the form (4.1), where 0.9 is a safety factor. Hence we obtain  $h$  as

$$h = \frac{0.9}{\sqrt{\max_{\Re(q_K) \geq r - \Delta r} \left( (\Re(q_K)/a_{\text{ell}})^2 + (\Im(q_K)/b_{\text{ell}})^2 \right)}}, \quad (4.2)$$

which then has to be bounded above by  $h_{\text{max}}$ , cf. (2.3).

Remark that this novel heuristic gives a larger steplength than heuristic (2.7) for any DDE system. Indeed, the  $h$  given by (4.2) is larger than

$$0.9 \frac{\text{rad}_{\text{circ}}}{\max |\Omega(r\vec{r}) \cap (\mathbb{C}^+ + r - \Delta r)|}. \quad (4.3)$$

The denominator of (4.3) is clearly smaller than the denominator used in heuristic (2.7). In order to assess the numerator of (4.3), assume e.g. that the BDF methods are used in heuristic (2.7). One then has to compare  $\text{rad}_{\text{circ}}$  for the 4<sup>th</sup> and 6<sup>th</sup> order methods (cf. Table 2) to  $\rho_{\text{LMS},\epsilon} \approx 0.57$  and  $\rho_{\text{LMS},\epsilon} \approx 0.70$ , respectively, for the BDF methods of the same orders (for  $\epsilon = 0.1$ ). Note that the latter values are remarkably smaller. Consequently, the novel heuristic (4.2) results in a larger steplength  $h$  than the old heuristic (2.7).

## 4.2 Dividing the interesting region

By using heuristic (4.2), a steplength  $h$  is obtained which can be used in the method to approximate the rightmost characteristic roots, cf. Section 2.1. The computationally most expensive step in this algorithm is the numerical solution of an eigenvalue problem of size  $N$ , cf. (2.4). As argued in the previous section, the size of this eigenvalue problem is always smaller than in case heuristic (2.7) would be used. However, if this eigenvalue problem is still too large to be treated, it can be “split” into different smaller ones in the following manner.

As mentioned in Section 3.1.1, it can be expected that the error in approximating a characteristic root  $\lambda$  is smallest close to the origin. Remark that, by classical results, the interpolation error, cf. (2.2), is also smallest close to the origin. Hence, by solving the eigenvalue problem presented in Section 2.1, one focuses on the characteristic roots  $\lambda$  in the neighborhood of the origin, i.e., they are approximated with a certain minimal accuracy. The size of this neighborhood grows with decreasing steplength  $h$ . Consider the “shifted system”, where  $A_0$  and  $A_j$ , for  $j = 1, \dots, m$ , in (1.1) are replaced by  $A_0 - \lambda_s I$  and  $A_j e^{-\lambda_s \tau_j}$ , respectively. The spectrum of this shifted system is obtained by translating the spectrum of the

original system by the (complex) value  $-\lambda_s$ . Hence by computing the spectra of shifted systems, one can focus on different parts of the spectrum of the original system.

Thus, instead of solving a single eigenvalue problem that “zooms in” on the origin, one can use the following alternative. First, choose a feasible size  $N$  of the eigenvalue problems and calculate the corresponding steplength  $h$ . Next, consider the interesting part of  $\mathbb{C}^+ + r$ , i.e., the intersection with (the estimation of)  $\Omega(r\vec{\tau})$ . For ease of use, we work with a rectangle with edges parallel to the coordinate axes that includes the points  $q_K$  in  $\Omega(r\vec{\tau}) \cap (\mathbb{C}^+ + r - \Delta r)$ , cf. Section 4.1. The part of this rectangle in  $\mathbb{C}^+ + r$  has to be covered by translated copies of the ellipse (4.1), scaled by  $0.9/h$ . Next, a collection of shifts  $\{\lambda_s\}$  corresponding to such a covering is determined. Finally, each shift  $\lambda_s$  is considered separately. Approximations  $\tilde{\lambda}$  to roots of the corresponding “shifted system” are computed (by solving a eigenvalue problem of the size determined above) and “shifted back” by adding  $\lambda_s$ . This approach is particularly appealing if solving a single eigenvalue problem would be intractable, e.g. in case of large-scale DDE systems. The above technique allows to “split” the single eigenvalue problem into several smaller (computationally feasible) ones. Each one “zooms in” on a different part of the spectrum.

### 4.3 Estimating the location of $\Omega(r\vec{\tau})$

We now briefly discuss how to compute (efficiently) a set of points  $\{q_K\}_{K \geq 1}$ , used in (4.2), that represents a good estimation of the location of  $\Omega(r\vec{\tau})$ . This information is needed to calculate the heuristic steplength (4.2).

**The general case.** In general, one can only resort to the definition of  $\Omega(\cdot)$  in (2.8) to obtain points  $q_K$ . This amounts to computing eigenvalues of matrices of the form

$$A_0 + \sum_{j=1}^m (A_j e^{-r\tau_j}) e^{-i\omega_j},$$

for a number of  $m$ -vectors  $\vec{\omega}$  chosen from  $[0, 2\pi]^m$ . These eigenvalue problems merely have size  $n$ , which is much smaller than the size  $N$  in (2.4). Therefore the computational cost to estimate the location of  $\Omega(r\vec{\tau})$  in this manner in case of one, two or three delays is negligible w.r.t. the total computational cost. However, this approach quickly becomes very expensive when the number of delays grows. Remark that the symmetry of  $\Omega(r\vec{\tau})$  w.r.t. the real axis can be exploited by choosing the  $m$ -vectors  $\vec{\omega}$  from the set  $[0, \pi] \times [0, 2\pi]^{m-1}$ .

The above procedure can be made adaptive by first computing a small number of points and only computing more according to a certain criterion. One criterion could be that the current maximum in (4.2) is reached for a point  $q$  with  $\Re(q) \gg r$ . Indeed, this would be unexpected considering the typical shape of the spectrum mentioned in Section 4.1.

Remark that computing (the boundary of)  $\Omega(r\vec{\tau})$  using variants of set-oriented (or path-following) techniques could be possible. For an application in another context, see e.g. [4]. Note though that  $\Omega(r\vec{\tau})$  does not have to be determined very accurately. Moreover, it is important to notice that in a continuation process, the steplength calculation using (4.2) does not have to be repeated for each steady state since some information can be reused.

**A special case.** Locating the  $\Omega_i(r\vec{\tau})$ -regions accurately in the complex plane is rather easy for certain systems. Here we consider the case where  $A_0, \dots, A_m$  can be transformed to upper (or lower) triangular form by the same nonsingular matrix  $X \in \mathbb{C}^{n \times n}$ , i.e.,  $A_j = XS_jX^{-1}$ , where all  $S_j \in \mathbb{C}^{n \times n}$  are upper (or lower) triangular,  $j = 0, \dots, m$ . Let  $[M]_{i,j}$  denote the element with indices  $(i, j)$  of a matrix  $M$ . Then it follows from (2.8) that  $\text{cl } \Omega_i((\mathbb{R}^+ + r)\vec{\tau})$  is the (closed) disc centered at  $[S_0]_{i,i}$  with radius  $\sum_{j=1}^m |[S_j]_{i,i}| e^{-r\tau_j}$ , for  $i = 1, \dots, n$ . One (important) class of matrices with this property are the tri-diagonal, symmetric Toeplitz matrices. These matrices have the same set of eigenvectors, regardless the value on the main diagonal or the value on the first upper and lower subdiagonal, see e.g. [12, Lemma 10.5]. These matrices can arise from, e.g. the space discretization by finite differences of a one-dimensional reaction-diffusion delay PDE that is linearized about a homogeneous steady state solution.

## 5 Examples

This section presents examples that illustrate the efficient computation of the characteristic roots for a small-scale and a large-scale DDE system. We show that the use of the novel heuristic (4.2) leads to a significant reduction of the computational cost compared to heuristic (2.7) from [8].

### 5.1 A small-scale system of DDEs

For a system of four DDEs and one delay,  $\tau = 1$ , with

$$A_0 = \begin{bmatrix} -1 & 0 & 0 & 0 \\ 0 & 1 & 0 & 0 \\ 0 & 0 & -10 & -4 \\ 0 & 0 & 4 & -10 \end{bmatrix} \quad \text{and} \quad A_1 = \begin{bmatrix} 3 & 3 & 3 & 3 \\ 0 & -1.5 & 0 & 0 \\ 0 & 0 & 3 & -5 \\ 0 & 5 & 5 & 5 \end{bmatrix}.$$

we computed roots  $\lambda \in \mathbb{C}^+ + r$  for  $r = 0, -0.5, -1, -3$ . We used, for comparison, the special-purpose methods of 4<sup>th</sup>, 6<sup>th</sup> and 8<sup>th</sup> order and the BDF methods of 4<sup>th</sup> and 6<sup>th</sup> order. The  $\Omega_i(r\vec{\tau})$ -regions in case  $r = 0$  are shown in Fig. 1 (left) and the quantities used in the steplength heuristics are given in Table 3. Table 4 lists the steplength  $h$  and the size  $N$  of the corresponding eigenvalue problem for the novel heuristic (4.2) with  $\Delta r = 0.1$  and for the old heuristic (2.7). If  $h > h_{\max} = \tau_{\min}/s_+$ , the steplength is set equal to  $h_{\max}$ . This is indicated by a (\*). In this case,  $N = n(3k - 1)$  for the special-purpose methods.

	$r = 0$	$r = -0.5$	$r = -1$	$r = -3$
$\ A_0\  +  r  + \sum_{j=1}^m \ A_j\  e^{-r\tau_j}$	21.1	28.3	39.9	221.7
$\max  \Omega(r\vec{\tau}) \cap (\mathbb{C}^+ + r - \Delta r) $	2.86	8.58	18.8	131.0

Table 3: Quantities used in the computation of the steplength for different  $r$ .

In order to assess the merits of the two adaptations (the location of  $\Sigma_\tau(\mathbb{C}^+ + r)$  w.r.t.  $\mathbb{C}^+ + r$  and the special-purpose LMS methods) Table 4 also lists the following quantities:

$r$	Order	old heuristic		adaptation 1		adaptation 2		new heuristic	
		$h$	$N$	$h$	$N$	$h$	$N$	$h$	$N$
0	4	$2.44 \times 10^{-2}$	184	$7.16 \times 10^{-2}$	68	$1.80 \times 10^{-1}$	44	$5.28 \times 10^{-1}$ (*)	20
	6	$2.97 \times 10^{-2}$	168	$8.95 \times 10^{-2}$	68	$2.19 \times 10^{-1}$	52	$4.84 \times 10^{-1}$ (*)	32
	8			$9.40 \times 10^{-2}$	72			$6.94 \times 10^{-1}$ (*)	44
-0.5	4	$1.82 \times 10^{-2}$	240	$5.33 \times 10^{-2}$	88	$6.01 \times 10^{-2}$	88	$1.77 \times 10^{-1}$	36
	6	$2.22 \times 10^{-2}$	216	$6.67 \times 10^{-2}$	80	$7.32 \times 10^{-2}$	88	$2.55 \times 10^{-1}$	36
	8			$7.00 \times 10^{-2}$	88			$2.32 \times 10^{-1}$	48
-1	4	$1.29 \times 10^{-2}$	332	$3.79 \times 10^{-2}$	120	$2.75 \times 10^{-2}$	168	$8.05 \times 10^{-2}$	64
	6	$1.57 \times 10^{-2}$	288	$4.74 \times 10^{-2}$	108	$3.34 \times 10^{-2}$	152	$1.12 \times 10^{-1}$	56
	8			$4.97 \times 10^{-2}$	112			$1.06 \times 10^{-1}$	68
-3	4	$2.33 \times 10^{-3}$	1740	$6.82 \times 10^{-3}$	600	$3.94 \times 10^{-3}$	1036	$1.15 \times 10^{-2}$	360
	6	$2.83 \times 10^{-3}$	1448	$8.53 \times 10^{-3}$	492	$4.79 \times 10^{-3}$	868	$1.01 \times 10^{-2}$	420
	8			$8.95 \times 10^{-3}$	476			$1.52 \times 10^{-2}$	292

Table 4: Values of the steplength  $h$  and size  $N$  of the eigenvalue problem for  $r = 0, -0.5, -1, -3$ . Left column: using the old heuristic (2.7) for the BDF methods. Mid columns: using the adaptations (5.1) resp. (5.2). Right column: using the new heuristic (4.2) for the special-purpose methods.

- “adaptation 1” : for the special-purpose LMS methods of 4<sup>th</sup>, 6<sup>th</sup> and 8<sup>th</sup> order:

$$h = 0.9 \frac{\text{rad}_{\text{circ}}}{\|A_0\| + |r| + \sum_{j=1}^m \|A_j\| e^{-r\tau_j}}, \quad (5.1)$$

where  $\text{rad}_{\text{circ}}$  is taken from Table 2.

- “adaptation 2” : for the BDF methods of 4<sup>th</sup> and 6<sup>th</sup> order:

$$h = 0.9 \frac{\rho_{\text{LMS},\epsilon}}{\max |\Omega(r\vec{\tau}) \cap (\mathbb{C}^+ + r - \Delta r)|}, \quad (5.2)$$

where  $\max |\Omega(r\vec{\tau}) \cap (\mathbb{C}^+ + r - \Delta r)|$  is given in Table 3.

Adaptation 1 (cf. (5.1)) is obtained by replacing  $\rho_{\text{LMS},\epsilon}$  in (2.7) by  $\text{rad}_{\text{circ}}$ . Hence it guarantees that  $\Sigma_\tau(\mathbb{C}^+ + r)$  belongs to  $\frac{1}{h}\text{LMS}(\mathcal{T}_\delta)$ . The resulting  $h$  benefits from the improvement by the special-purpose LMS methods, but still uses an overestimate in the denominator which severely restricts the steplength. Adaptation 2 (cf. (5.2)) uses a more realistic bound for  $|\Sigma_\tau(\mathbb{C}^+ + r) \cap (\mathbb{C}^+ + r)|$ . However, as mentioned before,  $\rho_{\text{LMS},\epsilon}$  is remarkably smaller than  $\text{rad}_{\text{circ}}$ . Table 4 illustrates that both adaptations are improvements to the old steplength heuristic. The new heuristic combines the merits of both adaptations.

Table 4 illustrates that  $h$  decreases with  $r$ . This is inevitable since the size of the  $\Omega_i(r\vec{\tau})$ -regions depends on  $r$  through  $e^{-r\tau_j}$ , for  $j = 1, \dots, m$ .

Table 5 gives ratio of the steplengths and the ratio of the sizes of the eigenvalue problems for the new heuristic and the old heuristic (2.7). Notice that the ratio  $N_{\text{old}}/N_{\text{new}}$  listed in Table 5 decreases with  $r$ . However, because  $N_{\text{old}}/N_{\text{new}} \gg 1$ , the novel heuristic is superior.

Fig. 4 shows the approximate roots  $\tilde{\lambda}$  with their corrections for the special-purpose methods of 4<sup>th</sup> and 6<sup>th</sup> order for  $r = -1, -3$ . Remark the good correspondence between an approximate root  $\tilde{\lambda}$  and the exact  $\lambda$ . This certainly holds for roots  $\tilde{\lambda}$  that lie in  $\frac{0.9}{h}\mathcal{T}_\delta$ , which is also indicated in Fig. 4. Notice that the rightmost part of the spectrum, which lies in the middle of  $\frac{0.9}{h}\mathcal{T}_\delta$  is approximated with a high accuracy.

Order		$r = 0$	$r = -0.5$	$r = -1$	$r = -3$
4	$h_{\text{new}}/h_{\text{old}}$	20.5	9.7	6.2	4.9
	$N_{\text{old}}/N_{\text{new}}$	9.2	6.7	5.2	4.8
6	$h_{\text{new}}/h_{\text{old}}$	11.2	11.5	7.1	3.6
	$N_{\text{old}}/N_{\text{new}}$	5.3	6.0	5.1	3.6

Table 5: Ratios of the steplengths  $h_{\text{new}}/h_{\text{old}}$  and ratios of the sizes of the eigenvalue problem,  $N_{\text{old}}/N_{\text{new}}$ , where  $h_{\text{new}}$  comes from heuristic (4.2) for special-purpose LMS methods and  $h_{\text{old}}$  from heuristic (2.7) for the BDF methods. For  $r = 0$ ,  $h_{\text{new}} > h_{\text{max}}$  and  $h_{\text{new}}$  is set to  $h_{\text{max}}$ .

## 5.2 A large-scale system of DDEs

In this section, a large-scale DDE system is considered. For comparison, we use the novel heuristic (4.2) with the special-purpose method of 6<sup>th</sup> order and heuristic (2.7) with the BDF method of 6<sup>th</sup> order.

The following hybrid DDE-PDE system models a semiconductor laser subject to conventional optical feedback and lateral carrier diffusion [14]. The system in the complex scalar variable  $A(t)$  and real  $Z(x, t)$ , where  $x \in [-0.5, 0.5]$ , reads as

$$\begin{aligned} \frac{dA(t)}{dt} &= (1 - i\alpha)A(t)\zeta(t) + \eta A(t - \tau)e^{-i\phi} - i b A(t), & (5.3) \\ T \frac{\partial Z(x, t)}{\partial t} &= d \frac{\partial^2 Z(x, t)}{\partial x^2} - Z(x, t) + P(x) \\ &\quad - F(x)(1 + 2Z(x, t))|A(t)|^2, & (5.4) \end{aligned}$$

where “ $i$ ” is the imaginary unit and

$$\zeta(t) = \frac{\int_{-0.5}^{0.5} F(x) Z(x, t) dx}{\int_{-\infty}^{\infty} F(x) dx}. \quad (5.5)$$

The functions  $P(x)$  and  $F(x)$  are specified in [14]. Zero Neumann boundary conditions for  $Z(x, t)$  are imposed at  $x = \pm 0.5$ . We fix parameters  $\alpha = 3$ ,  $\phi = 0$ ,  $T = 1000$ ,  $d = 1.68 \times 10^{-2}$  and delay  $\tau = 1000$ . For the numerical computations, the time variable is rescaled as  $t \leftarrow 1000 t$ . The symmetry about  $x = 0$  is exploited by considering only the interval  $[0, 0.5]$ . We split (5.3) into real and imaginary part and discretize (5.4) in space using a second order central difference formula with constant stepsize  $\Delta x = 0.5/128$ . Moreover, (5.5) is approximated using the trapezoidal quadrature rule. Hence the resulting DDE system has size 131. This system is linearized about the steady state solution with  $|A| \approx 1.8209$  and  $b \approx 1.1119 \times 10^{-3}$ .

For  $\eta \approx 2.5717 \times 10^{-3}$ , there is a Hopf bifurcation point. For this point, Fig. 5 shows approximate roots  $\tilde{\lambda}$  and their corrections. The same conclusions concerning the accuracy hold as for the previous example. Note that, due to the rotational symmetry in the complex variable  $A$ , there is always an additional characteristic root at zero.

The spectrum shown in Fig. 5 was computed using  $r = -1$ ,  $\Delta r = 0.1$  and  $\delta = 0.1$  (left) and  $\delta = 0.01$  (right). For this example, contrary to the previous

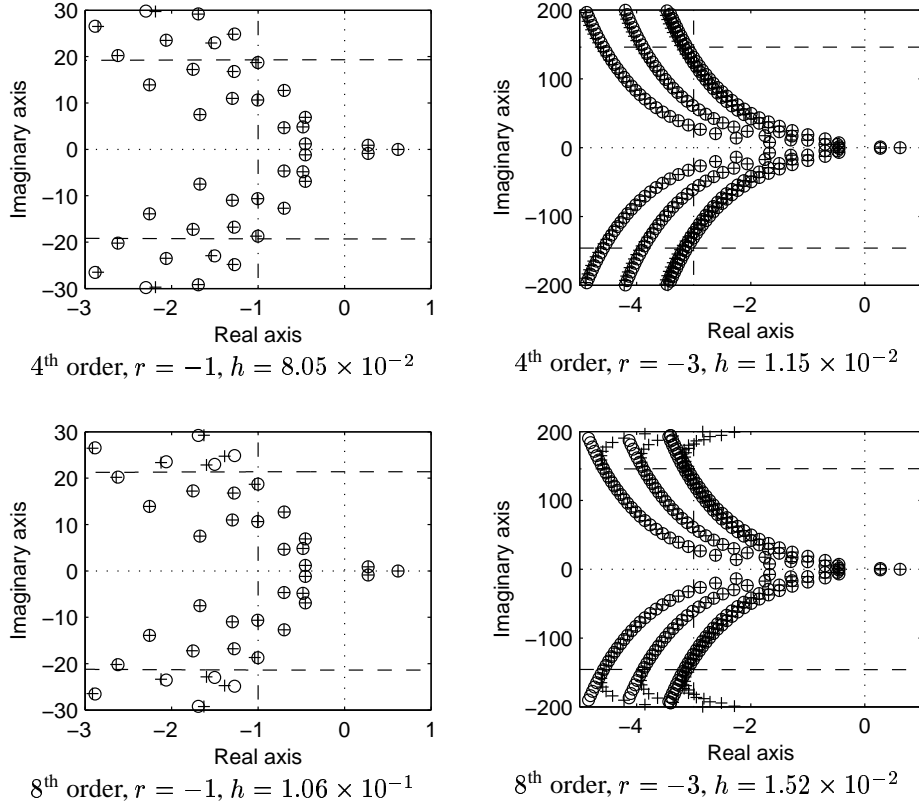


Figure 4: For the first example in Section 5.1: approximate roots  $\tilde{\lambda}$  (+), their corrections using Newton iterations (o). Top: BDF method of 4<sup>th</sup> order. Mid and bottom: special-purpose methods,  $\frac{0.9}{h}\mathcal{T}_\delta$  (bounded by the dashed line).

one, we use a steplength  $h$  commensurate with  $\tau$ . That is, the value of  $h$  obtained from heuristic (4.2) is lowered to obtain that  $\tau/h$  is an integer value. This allows us to avoid the interpolation for the delayed term in (2.9). Heuristic (4.2) gives  $h = \tau/24$  ( $N = 3537$ ) in case  $\delta = 0.1$  and  $h = \tau/36$  ( $N = 5109$ ) in case  $\delta = 0.01$ . The resulting eigenvalue problems are large, but still feasible. Heuristic (2.7) gives  $h = \tau/7195$  which leads to  $N = 943331$  (for  $\epsilon = 0.1$ ); hence, this eigenvalue problem is intractable.

The steplength resulting from heuristic (2.7) is so small because  $\|A_0\| + |r| + \sum_{j=1}^m \|A_j\| e^{-r\tau_j} \approx 4531.8$  severely overestimates  $\max |\Omega(r\vec{\tau}) \cap (\mathbb{C}^+ + r)| \approx 52.5$ . The former value is large because the  $\Omega_i(r\vec{\tau})$ -regions extend far to the left in  $\mathbb{C}^-$ . However, only the extent of  $\Omega(r\vec{\tau})$  in  $\mathbb{C}^+ + r$  is important, cf. Section 2. For space discretizations of reaction-diffusion systems, the tail of  $\Omega_i(r\vec{\tau})$ -regions will typically grow to the left when the discretization in space becomes finer. Indeed, in this case, the real part of the leftmost eigenvalues of  $A_0$  typically tends to minus infinity.

Remark that use of the  $\Omega_i(r\vec{\tau})$ -regions ensures that the Hopf bifurcation point, shown in Fig. 5, caused by roots with large imaginary part, is not “missed”. Such roots could be missed without insight in the location of characteristic roots, as presented in [15].

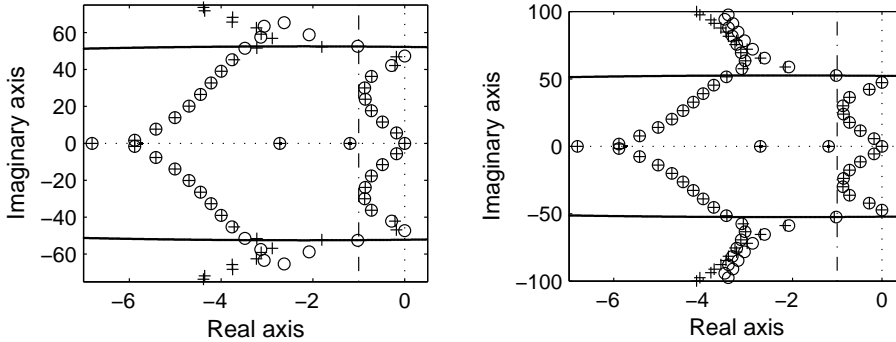


Figure 5: The large-scale DDE system of Section 5.2 with  $r = -1$ , using the 6<sup>th</sup> order special purpose method: The approximate roots  $\tilde{\lambda}$  (+) and their corrections ( $\circ$ ) and  $\Omega(r\vec{\tau})$  (solid line) in case  $\delta = 0.1$  (left) and in case  $\delta = 0.01$  (right).

Finally, consider the technique of “dividing the interesting region”, cf. Section 4.2. We will split the single eigenvalue problem of size  $N = 5109$  (for  $\delta = 0.01$ ) into smaller ones. In this case, the points  $q_K$  in  $\Omega(r\vec{\tau}) \cap (\mathbb{C}^+ + r - \Delta r)$  belong to a rectangle with right, upper vertex  $12.64 + i52.43$ . For the choice  $N = 2620$  (corresponding to  $h = \tau/17$ ), two eigenvalue problems have to be solved: one (real) eigenvalue problem (corresponding to a shift  $\lambda_s = 0$ ) and one (complex) eigenvalue problem (corresponding to a shift  $\lambda_s = i34.95$ ).

## 6 Conclusions

In [8], a method was proposed for the computation of the rightmost characteristic roots  $\lambda$  with  $\Re(\lambda) \geq r \in \mathbb{R}$ . These roots determine the stability (of the zero steady state solution) of a linear DDE system (1.1). The proposed approach is based on the discretization of the solution operator to (1.1) over one time step by a linear multistep (LMS) method combined with polynomial interpolation of the delayed terms. This leads to a large eigenvalue problem whose size is inversely proportional to the steplength used in the discretization.

In this paper, we have presented a modification to this procedure. The novel procedure is more efficient while maintaining the reliability of the numerical results. To achieve this goal, we have used theoretical foundations on the location and numerical preservation of roots obtained in [15]. Furthermore, we have constructed special-purpose LMS methods instead of using methods traditionally used for time integration. These techniques allow to use a novel heuristic resulting in a larger steplength, hence the size of the resulting eigenvalue problem is reduced. We showed that, if this eigenvalue problem is still too large to be treated, it can be “split” into different smaller ones which “zoom in” unto different pieces of the complex plane. The resulting procedure computes efficiently and accurately *all* characteristic roots  $\lambda$  with  $\Re(\lambda) \geq r$ . In particular, no roots with large imaginary parts can be overlooked.

The performance of the new procedure was demonstrated for a small- and a large-scale system of DDEs.

## Acknowledgments

This research presents results of the Project IUAP P5/22 funded by the Interuniversity Attraction Poles Programme - Belgian Science Policy. The scientific responsibility rests with the authors. K.V. is a Research Assistant of the Fund for Scientific Research - Flanders (Belgium).

## References

- [1] D. BREDÁ, *The infinitesimal generator approach for the computation of characteristic roots for delay differential equations using BDF methods*, Research Report RR02/17UDMI, Department of Mathematics and Computer Science, University of Udine, 2002.
- [2] D. BREDÁ, S. MASET, AND R. VERMIGLIO, *Pseudospectral differencing methods for the numerical computation of characteristic roots for delay differential equations*, Research Report RR03/01UDMI, Department of Mathematics and Computer Science, University of Udine, 2003.
- [3] ———, *Computing the characteristic roots for delay differential equations*, IMA J. Numer. Anal., 24 (2004), pp. 1–19.
- [4] M. DELLNITZ AND O. JUNGE, *Set oriented numerical methods for dynamical systems*, in Handbook of dynamical systems, B. Fiedler, ed., vol. 2, North-Holland, 2002, ch. 5, pp. 221–264.
- [5] K. ENGELBORGHES, T. LUZYANINA, AND D. ROOSE, *Numerical bifurcation analysis of delay differential equations*, J. Comput. Appl. Math., 125 (2000), pp. 265–275.
- [6] K. ENGELBORGHES, T. LUZYANINA, AND D. ROOSE, *Numerical bifurcation analysis of delay differential equations using DDE-BIFTOOL*, ACM Trans. Math. Softw., 28 (2002), pp. 1–21.
- [7] K. ENGELBORGHES, T. LUZYANINA, AND G. SAMAËY, *DDE-BIFTOOL v. 2.00: a Matlab package for numerical bifurcation analysis of delay differential equations*, Report TW 330, Department of Computer Science, K.U.Leuven, Leuven, Belgium, 2001. Available from <http://www.cs.kuleuven.ac.be/~koen/delay/ddebiftool.shtml>.
- [8] K. ENGELBORGHES AND D. ROOSE, *On stability of LMS methods and characteristic roots of delay differential equations*, SIAM J. Numer. Anal., 40 (2002), pp. 629–650.
- [9] E. HAIRER, S. P. NORSETT, AND G. WANNER, *Solving ordinary differential equations. I.: Nonstiff problems*, vol. 8 of Springer series in computational mathematics, Springer Berlin, 2nd ed., 1993.
- [10] E. HAIRER AND G. WANNER, *Solving ordinary differential equations. II: Stiff and differential-algebraic problems*, vol. 14 of Springer series in computational mathematics, Springer Berlin, 2nd ed., 1996.

- [11] J. HALE AND S. M. VERDUYN LUNEL, *Introduction to Functional Differential Equations*, vol. 99 of Applied Mathematical Sciences, Springer-Verlag, 1993.
- [12] A. ISERLES, *A first course in the numerical analysis of differential equations*, Cambridge Texts in Applied Mathematics, Cambridge University Press, 1996.
- [13] G. STÉPÁN, *Retarded dynamical systems: stability and characteristic functions*, vol. 210 of Pitman Research Notes in Mathematics Series, Longman Scientific & Technical, 1989.
- [14] K. VERHEYDEN, K. GREEN, AND D. ROOSE, *Numerical stability analysis of a large-scale delay system modelling a lateral semiconductor laser subject to optical feedback*, Phys. Rev. E, (2003). accepted.
- [15] K. VERHEYDEN, T. LUZYANINA, AND D. ROOSE, *Location and numerical preservation of characteristic roots of delay differential equations by LMS methods.*, Technical Report TW-382, Department of Computer Science, K.U.Leuven, Leuven, Belgium, Dec. 2003. submitted.